

**$^{79}\text{Br}$  and  $^{81}\text{Br}(p, xn)$  and  $(p, pxn)$  excitation functions in the energy range 10–85 MeV**

M. Dikšić, J.-L. Galinier,\* H. Marshall, and L. Yaffe

*Department of Chemistry, McGill University, Montreal, P.Q. H3A 2K6, Canada*

(Received 17 October 1978)

A study of  $(p, xn)$  and  $(p, pxn)$  reactions on  $^{79}\text{Br}$  and  $^{81}\text{Br}$  was made. The excitation functions were measured in the energy range 10–85 MeV. The excitation functions experimentally obtained were compared with those predicted by intranuclear cascades and two pre-equilibrium models followed by equilibrium evaporation. None of the three computer codes was able to reproduce all excitation functions satisfactorily. The relative success of the computer codes tested is discussed.

NUCLEAR REACTIONS  $^{79}\text{Br}(p, n)$ ,  $(p, 3n)$ ,  $(p, 4n)$ ,  $(p, pn)$ ,  $(p, p2n)$ ,  $(p, p3n)$ ,  $(p, p4n)$ ,  $(p, p5n)$ ,  $^{81}\text{Br}(p, 3n)$ ,  $(p, 5n)$ ,  $(p, 6n)$ ,  $(p, pn)$ ,  $(p, p3n)$ ,  $(p, p4n)$ ,  $(p, p5n)$ ,  $(p, p6n)$ , enriched target,  $E=10\text{--}85$  MeV, measured  $\sigma(E)$ .

## I. INTRODUCTION

During the past two decades many studies have been made on  $(p, xn)$  and  $(p, pxn)$  reactions in the medium-energy range. However, sets of experimental excitation functions for several  $(p, xn)$  and  $(p, pxn)$  reactions on the same target nucleus, with  $x \leq 2$ , are rare. It is in this region that the reaction mechanism gradually changes from almost pure compound-nucleus formation to a mechanism involving pre-equilibrium emission of particles from a complex system.<sup>1</sup> Several models have been proposed for these reactions, each describing the reaction in terms of a two-step cascade (pre-equilibrium)-evaporation process. A number of Monte-Carlo treatments of the cascade step, based on different nuclear models, have been made.<sup>2–4</sup> In recent years, several pre-equilibrium models,<sup>5,6</sup> based on the work of Griffin,<sup>7</sup> have been proposed for the calculation of reaction excitation functions in this energy region.

To date, the most widely tested intranuclear cascade model (INC) has been VEGAS.<sup>4</sup> It uses a non-uniform nucleon density distribution and considers reflection and refraction at the surface of changing potential. The combination of INC and the evaporation code of Dostrovsky et al.<sup>8</sup> yields reaction cross sections which may then be compared with experimental results. However, this combination was not able to reproduce excitation functions well, either in shape or magnitude (see eg. refs. 9,10).

Bertini's INC model<sup>3</sup> (MECC-7) combined with Dresner's evaporation code<sup>11</sup> (I4C) has not been tested extensively at energies below 100 MeV. This model was able to reproduce quite well the non-elastic cross section for proton-induced reactions<sup>12</sup> at energies 30–60 MeV, and quite well the shapes and magnitude of proton spectra at several angles from 39- and 62-MeV protons on various target elements.<sup>13</sup> The model also had some success in describing the excitation functions of proton-induced reactions in the energy range 10–85 MeV.<sup>14,15</sup> The two pre-equilibrium codes most widely used are, Blann's<sup>5</sup> geometry-

dependent hybrid model, and Gadioli's<sup>6</sup> exciton codes. The first performs calculations in closed form, whereas the second uses average transition rates. It has been suggested<sup>16,17</sup> that, in the latter case, an increase of the mean free paths by a factor of  $\sqrt{4}$  is necessary in order to get reasonable reaction cross sections.

Lately, the exciton model was widely tested in the prediction of the excitation functions for proton-induced reactions<sup>18,19</sup> on nuclei with mass  $A \approx 90$  and 200. In the opinion of the authors, it reproduced all studied excitation functions satisfactorily, provided the mean free paths of nucleons was four times longer than that derived from free nucleon-nucleon scattering cross sections.

In this paper we report the experimental reaction cross sections for  $^{79}\text{Br}(p, xn)$  ( $x=1,3,4$ ) and  $(p, pxn)$  ( $x=1-5$ ), and  $^{81}\text{Br}(p, xn)$  ( $x=3,5,6$ ) and  $(p, pxn)$  ( $x=1,3-6$ ) reactions in the energy range 10–85 MeV. Only one of these excitation functions,  $^{81}\text{Br}(p, pn)$ , has been measured previously<sup>20</sup> in this energy range. The experimental excitation functions were compared with those predicted by Bertini's INC model followed by the equilibrium evaporation, pre-equilibrium exciton and geometry-dependent hybrid models in combination with equilibrium evaporation. We feel that this direct comparison of different models on a large set of competing reactions should be, at the least, a test of their relative success in describing the type of reaction mechanism which takes place in this energy range.

## II. EXPERIMENTAL

Irradiations were carried out in the internal circulating beam of the McGill Synchrocyclotron. The targets were placed at appropriate radii to get the desired proton energy. The uncertainty in the beam energy was  $\pm 2$  MeV. The irradiation times were 1–5 minutes. The target, consisting either of enriched  $^{79}\text{Br}$  or  $^{81}\text{Br}$ , was enclosed in thin-walled aluminum tubing, the tube ends sealed

TABLE I. Nuclear data for nuclides measured

Isotope	$t_{1/2}$	$E_{\gamma}$ (keV)	$I_{\gamma}\%$ <sup>a</sup>	Ref.
<sup>79</sup> Kr	35.04 h	261.3	12.7	46
		398.0	9.5	
<sup>77</sup> Kr	74.7 min	129.0	87.3	47
		146.4	40.9	
<sup>76</sup> Kr	14.8 h	270.2	26.7	48
		315.7	40.0	
<sup>80</sup> Br <sup>m</sup> <sup>b</sup>	4.42 h	616.2	6.7	49
<sup>80</sup> Br <sup>g</sup>	17.4 min	616.2	6.7	49
<sup>78</sup> Br	6.46 min	614.0	13.6	50
<sup>77</sup> Br	56 h	238.9	26.0	47
		520.7	23.2	
<sup>76</sup> Br	16.2 h	559	72.4	48
		657.2	15.5	
<sup>75</sup> Br	98 min	286.5	92.0	51
<sup>74</sup> Br <sup>c</sup>	41.5 min	634.8	63	52
<sup>63</sup> Zn	38.0 min	669.6	8.47	53
		961.9	6.68	
<sup>24</sup> Na	15.0 h	1368.5	99.99	54
		2753.9	99.9	

<sup>a</sup>Number of gamma rays per 100 decays

<sup>b</sup>Daughter activity measured

<sup>c</sup>Only one isomer was measured

under pressure and flattened to an absorption thickness of about 0.8 MeV and 2 MeV at 50 and 10 MeV respectively. The isotopic composition of the enriched targets was (95.06±0.60)% and (97.81±0.05)% for <sup>79</sup>Br and <sup>81</sup>Br, respectively.

After irradiation, the entire target was usually mounted on a card for activity measurements. Description of target material and monitor reactions used in this work have been given elsewhere.<sup>21</sup>

The full-energy peaks (FEP) and intensities used in the estimation of the cross sections are given in Table I.

Activities were measured using a 30 cm<sup>3</sup> Ge(Li) detector coupled to a 4096-channel pulse-height analyser and the spectra were recorded on magnetic tape. The resolution of the system (full-width at half-maximum) was 2.8 keV at 1.33 MeV. Activities were followed for a period of at least one half-life. The constancy of the half-lives observed for the Kr isotopes (specially <sup>77</sup>Kr) was taken as proof that no loss of Kr occurred during the activity measurements. The area of the FEP was estimated by the computer code GAMANAL<sup>22</sup> and decay-curve analysis subsequently performed by means of the CLSQ computer code.<sup>23</sup> Counting rates at the end of irradiation were converted to disintegration rates by correcting them for gamma-ray intensity, detector efficiency and number of atoms for a particular target isotope. When several  $\gamma$ -rays belonging to the same nuclide were used to calculate disintegration rates, good agreement was obtained between these determinations (<6% difference), and the weighted average was taken as the experimental value. The formation cross sections for each nuclide were calculated from disintegration rates by means of standard equations and using the reaction

TABLE II. Monitor cross sections.

$E_p$ (MeV)	<sup>63</sup> Cu(p,n) <sup>63</sup> Zn <sup>a</sup> (mb)	<sup>27</sup> Al(p,3pn) <sup>24</sup> Na <sup>b</sup> (mb)	<sup>63</sup> Cu(p,2n) <sup>62</sup> Zn <sup>c</sup> (mb)
10	413		
15	315		
20	63		
25	33		197
30	43 <sup>d</sup>		132
35	54 <sup>d</sup>		47.5 <sup>e</sup>
40	54 <sup>d</sup>		15.5 <sup>e</sup>
45	29 <sup>d</sup>		11.8 <sup>e</sup>
50	22 <sup>d</sup>	5.3±0.3	
55		9.2±0.6	
60		9.9±0.6	
65		18 ±1	
70		12 ±1	
75		14 ±1	
80		12 ±1	
85		13 ±1	

<sup>a</sup>Reference 25 up to 25 MeV and reference 26 between 30 and 50 MeV. The latter were normalized as described in text.

<sup>b</sup>Reference 27.

<sup>c</sup>Reference 26, normalized as described in text, (error assumed 15%).

<sup>d</sup>Represents <sup>63</sup>Cu(p,n) + <sup>65</sup>Cu(p,3n) for natural copper, (error assumed ±15%).

<sup>e</sup>Represents <sup>63</sup>Cu(p,2n) + <sup>65</sup>Cu(p,4n) for natural copper, (error assumed ±15%).

$^{81}\text{Br}(p, pn)^{80}\text{Br}^m$  as an internal monitor. The cross sections for this reaction were measured in the first series of runs, as described in ref. 21. Several measurements were made at each energy. The cross sections for the primary monitors involved are given in Table II. The monitor cross sections for  $^{63}\text{Zn}$  and  $^{62}\text{Zn}$  production were normalized to the most recent  $^{12}\text{C}(p, pn)^{11}\text{C}$  monitor cross section data.<sup>24</sup> The individual cross sections were read from the smooth curve in the case of  $^{63}\text{Zn}$  and  $^{62}\text{Zn}$ , whereas those for  $^{24}\text{Na}$  were taken as given in ref. 27. In the energy range above 45 MeV where  $^{27}\text{Al}(p, 3pn)^{24}\text{Na}$  was used, the  $^{24}\text{Na}$  contribution by recoil from the Al tube was determined by running a blank experiment. This contribution was found to be negligible.

### III. RESULTS AND DISCUSSION

#### A. Experimental results

The formation cross sections for  $(p, xn)$  and  $(p, pxn)$  reactions measured in this work, relative to the formation cross section of the monitor reaction, are given in Tables III and IV. The contribution to the cross sections for  $^{79}\text{Br}$  have been corrected for the contribution from reactions on  $^{81}\text{Br}$  and vice-versa. The experimental excitation functions are shown in Figures 2-12 together with the theoretical fits. The uncertainties quoted are estimated total errors calculated as the square root of the sum of the squares of individual errors. These consist of the error associated with integration of FEP (which is reflected in the uncertainty in disintegration rates obtained from the analysis of the decay curves) and the error in monitor cross sections. All other errors were relatively small and consequently were not included, as described in ref. 15.

The results of this work may be compared with some previous measurements on  $^{79}\text{Br}$  and  $^{81}\text{Br}$ . The cross sections for  $^{81}\text{Br}(p, pn)$  reaction measured by Meadows<sup>20</sup>

and normalized to the most recent  $^{12}\text{C}(p, pn)^{11}\text{C}$  monitor cross section data<sup>24</sup> are in good agreement with ours. The only other measurements in the energy range studied in this work are  $^{79}\text{Br}(p, n)^{79}\text{Kr}$  at 12 MeV<sup>28</sup> and 3-25 MeV.<sup>29</sup> Within the quoted error they agree well with our results. The former one was normalized to the most recent monitor cross section data.<sup>24</sup> The measurements of Strohal and Caretto<sup>30</sup> on  $^{81}\text{Br}$  in the higher energy range of 250-440 MeV are in line with trend observed for this reaction in the present work.

#### B. Calculated cross sections

The experimental excitation functions have been compared with those predicted by a Monte-Carlo intranuclear cascade-evaporation<sup>3,11</sup> (MECC-7-I4C), pre-equilibrium geometry-dependent hybrid<sup>5,31</sup> (EVA-GDH)<sup>32</sup> and Gadioli's exciton<sup>6</sup> models.

The following constants were used in all three sets of calculations; radius parameter  $r_0 = 1.5 \times 10^{-13}$  cm and the level-density parameter  $a = A/10$ .

The binding energies used in the EVA-GDH and MECC-7-I4C computer codes were calculated from Meyers and Swiatecki<sup>33</sup> and pairing energies were taken from Cameron.<sup>34</sup> Gadioli's exciton code uses experimental binding energies<sup>35</sup> whenever possible or values calculated from Meyers and Swiatecki<sup>33</sup> when experimental data are missing. The pairing energies used in this latter code are those of Nemirovski and Adamchuk.<sup>36</sup>

The output from INC(MECC-7) was used as input into the evaporation code I4C.<sup>11</sup> The MECC-7 code uses a non-zero Fermi-type charge-distribution function<sup>37</sup> as an approximation for the nucleus. Three concentric spheres were used to that effect. The radii of the spheres were determined by the distances at which the function mentioned above reaches a fraction of the central density<sup>3</sup> equal to 0.9, 0.2, and 0.01, respectively. The neutron-to-proton

TABLE III. Experimental cross sections for  $^{79}\text{Br}$ .

$E_p$ (MeV)	$\sigma$ (mb)							
	(p,n)	(p,3n)	(p,4n)	(p,pn)	(p,p2n)	(p,p3n)	(p,p4n)	(p,p5n)
10	690±60							
15	490±58							
20	60±6			170±18	1.8± 1.1			
25	65±8	2.9± 1.0		230±24	84 ±10			
30		53 ± 6		180±20	140 ±16			
35	32±3	260 ±31	0.5±0.4	160±18	310 ±37	4.3± 1.6		
40	22±2	230 ±30	11 ±2	190±21	290 ±31	47 ± 6	1.5± 1.0	
45	24±2	130 ±16	31 ±5	180±20	290 ±34	150 ±17	2.1± 1.1	
48		130 ±14	42 ±5					
55	15±2	54 ± 7	38 ±5	190±22	240 ±26	240 ±26	42 ± 5	
60	16±2	42 ± 5	31 ±4	170±18	160 ±18	210 ±23	81 ± 9	0.6±0.4
65	13±1	35 ± 4	19 ±3	140±15	140 ±16	170 ±19	100 ±11	5.2±1.8
75	12±1	24 ± 3	13 ±2	160±25	120 ±14	100 ±11	82 ± 9	9.0±2.0
85	8±1	17 ± 2	9 ±1	130±14	80 ±10	90 ±10	60 ± 8	12 ±3

TABLE IV. Experimental cross sections for  $^{81}\text{Br}$ 

$E_D$ (MeV)	$\sigma$ (mb)								
	(p,3n)	(p,5n)	(p,6n)	(p,pn) <sup>a</sup>	(p,pn) <sup>b</sup>	(p,p3n)	(p,p4n)	(p,p5n)	(p,p6n)
15				17±3	23±3				
20				40±4	60±7				
25	140±15			54±6	110±11				
30	480±51			72±8	130±13				
35	440±47			66±7	120±13	6.1± 1.2			
40	370±39			70±7	110±11	44 ± 5			
45	220±22	3.5±1.1		67±7	110±12	160 ±17	4.5± 2.2		
55	110±11	28 ±4		73±5	100±7	260 ±26	96 ±12	3.3± 1.0	0.1 <sup>+0.2</sup> -0.09
60	80±15	41 ±6							
65	50±4	32 ±4	0.47±0.3	74±5	96±7	210 ±18	110 ±14	13 ± 2	0.3±0.2
75	53±6	33 ±4	6.0 ±2.1	66±5	85±6	140 ±16	120 ±13	64 ±10	5.3±1.1
85	35±4	19 ±2	7.5 ±1.5	66±5	77±5	120 ±10	100 ± 9	70 ± 9	20 ±3

a  $^{80}\text{Br}^g$ b  $^{80}\text{Br}^m$ 

density ratio in each region was taken equal to the neutron-to-proton ratio in the nucleus. The neutron-proton, proton-proton and nucleon-nucleon cross sections used in the calculation were those supplied along with the code, and were taken from the compilation of Hughes and Schwartz,<sup>38</sup> Beretta et al.<sup>39</sup> and Hess<sup>40</sup> respectively.

The evaporation code I4C written by Dresner<sup>11</sup> is based on Weisskopf's evaporation theory<sup>41</sup> and the work of Dostrovsky.<sup>8</sup> A more detailed description of this model can be found in the literature.<sup>2,3,11,13</sup>

A total of 2000 incident particle histories at 5 MeV intervals between 10 and 85 MeV was compiled. This gave good statistical accuracy to the calculated cross sections considered in this work. The standard deviation of the calculated cross sections was usually less than 5%. The excitation functions with a large number of nucleons in the exit channel, e.g.  $^{81}\text{Br}(p,6n)$  have standard deviations of about 20% around the maximum and about 40% at the rise of the excitation function. The comparison between experimental and calculated excitation functions will be discussed later.

The geometry-dependent hybrid model EVA-GDH is based on the work of Griffin.<sup>7</sup> In this model the pre-equilibrium decay has been formulated<sup>5,16</sup> as:

$$\left(\frac{d\sigma}{d\epsilon}\right)_v = \pi\pi^2 \sum_{\ell=0}^{\infty} (2\ell + 1) T_{\ell} \frac{\bar{n}}{\sum_{n=n_0}^{\bar{n}} n} P_v(\epsilon)$$

where

$$\frac{\bar{n}}{\sum_{n=n_0}^{\bar{n}} n} P_v(\epsilon) d\epsilon = \sum_{n=n_0}^{\bar{n}} \left[ \frac{\rho_{p,h}(U,\epsilon) g d\epsilon}{n^p \rho_{p,h}(E)} \right]$$

$$\left[ \frac{\lambda_c(\epsilon)}{\lambda_c(\epsilon) + \lambda_+(\epsilon)} \right] D_n$$

The quantity in the first set of square brackets gives the number of particles,  $v$ , which have energies between  $\epsilon$  and  $\epsilon + d\epsilon$ , whereas the quantity in the second set of brackets gives the fraction of those particles at energy  $\epsilon$  that are

emitted into the continuum.  $D_n$  represents the fraction of the reaction cross section surviving decay prior to reaching the  $n$  exciton configuration.  $\lambda_c(\epsilon)$  and  $\lambda_+(\epsilon)$  are the transition rates into the continuum of a particle with energy  $\epsilon$  and the rate at which a particle makes intranuclear transitions to  $(n+2)$  particle-hole states, respectively.  $\rho_{p,h}(E)$  and  $\rho_{p,h}(U,\epsilon)$  are the densities of exciton states with  $p$  particles plus  $h$  holes. The density of  $n=p+h$  states is arranged such that one exciton, if emitted, would have channel energy  $\epsilon$ , having a residual excitation of  $U = E - B_v - \epsilon$  distributed between  $n-1$  excitons, respectively.  $E$  is the excitation energy of the nucleus,  $B_v$  the binding energy of particle  $v$ , and  $\epsilon$  its kinetic energy, and  $g$  is the single nucleon density. The factor  $n^p$  is the number of excitons that are nucleons of type  $v$  and  $\pi = \lambda/2\pi$ , where  $\lambda$  is the de Broglie wavelength. The neutron or proton single particle state densities have been defined by Fermi gas values and are given with detailed evaluation of other quantities in ref. 5, 31, and 42. The intra-nuclear transition rates also are given in ref. 5. It can be shown that these parameters are functions of nuclear densities and/or potential well depth. To consider any resultant changes which would occur in the hybrid model one considers contributions from zones of the nucleus, where the population of each zone is determined by the transmission coefficients ( $T_{\ell}$ ) for the partial waves in these zones. A Fermi density distribution<sup>28</sup> was used to define the density in each zone. The density-dependent parameters are averaged along the projectile paths corresponding to each partial wave. The transmission coefficients are taken from ref. 43.  $n^p_v(\epsilon)$  is the probability of emitting a nucleon of type  $v$  with energy  $\epsilon$  from an exciton state,  $n$ . The equilibrium part of the cross section was calculated by using Dostrovsky's evaporation model.<sup>8</sup>

In our calculations we used an initial

number of excitons equal to 3, a probability of having a proton in an excited state (EX2) was varied between 1.1 and 1.4, and the mean-free-path multiplication factor C was set at 2. The latter modifies the mean-free-path based on free nucleon-nucleon scattering cross sections. The cross sections, calculated with EX2=1.2, EX1=0.8, and C=2, are compared with the experimental results.

According to its authors<sup>18,19</sup> the exciton model has now reached the stage where the level-density parameter, a, is the only freely varying parameter in the calculation of (p,xn) and (p,pxn) cross sections. It is based on the works of Griffin<sup>7</sup> and Williams.<sup>44</sup> The cross section for pre-compound emission is given by<sup>6</sup>

$$\sigma_{\alpha\beta}^{\sigma} = \sigma_R(\alpha) \left\{ \frac{W_c^{n_0}}{W_c^{n_0} + W_{eq}^{n_0}} \frac{W_c^{n_0}}{W_c^{n_0}} + \frac{\bar{n}}{\sum_{n=n_0+2}^{n_0+2} \left[ \prod_{j=n_0}^{n-2} \frac{W_{eq}^j}{W_c^j + W_{eq}^j} \right]} \frac{W_c^n}{W_c^n + W_{eq}^n} \frac{W_c^n}{W_c^n} \right\}$$

$$\Delta n = +2 \quad \Delta n = +2$$

where  $\sigma_R(\alpha)$  denotes the reaction cross section,  $n_0$  the initial number of excitons,  $W_c^n$  the probability per unit time of emitting one particle into the continuum,  $W_{eq}^n$  the probability per unit time of the two-body interaction inside the nucleus having a number of excitons  $n+2$ ,  $\bar{n}$  is the average exciton number at equilibrium,  $W_{c\beta}^n/W_c^n$  and  $W_{c\beta}^{n_0}/W_c^{n_0}$  are branching ratios for the emission of particle  $\beta$ . A semi-empirical equation of Francis and Watson<sup>45</sup> was used to calculate the total reaction cross sections,  $\sigma_R$ , used in both the EVA-GDH and exciton codes.

The cross section for the emission of a particle  $\nu$  at equilibrium was based on a modification<sup>19</sup> of the Monte-Carlo model of Dostrovsky et al.<sup>8</sup>

The calculation of  $W_{eq}^n$  requires a knowledge of the value of the average mean free path<sup>6,19</sup> and was taken as four times the value calculated from the nucleon-nucleon scattering cross sections, as suggested by the authors of the code.<sup>6</sup> The calculation of these probabilities has been described in the literature.<sup>6,19</sup> A total of 5000 cascades was run at each energy. This gave a standard deviation of less than 5% for calculated cross sections for the large majority of excitation functions. The standard deviations for the calculated excitation functions for the reaction <sup>81</sup>Br(p,6n) are about 10% and 20% for the maximum and the rise of the functions respectively.

It is important to emphasize that the Bertini program<sup>3,12,13</sup> uses total reaction cross sections (see Figure 1) which are different from the Francis-Watson values used by the EVA-GDH and exciton codes. Bertini's program uses total reaction cross sections which however are not much

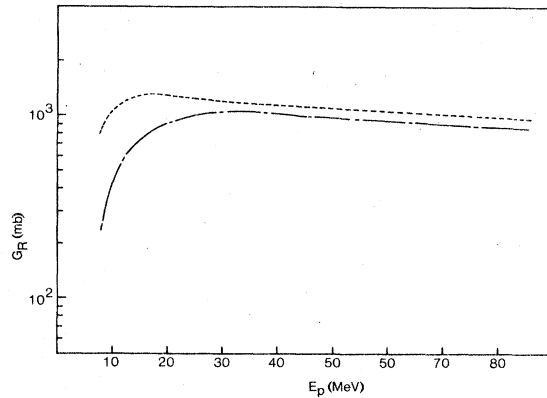


FIG. 1. Total reaction cross section for <sup>79</sup>Br as a function of proton bombardment energy.

--- calculated by use of INC code  
 — calculated by use of Francis and Watson equation

See text for further details.

different from the estimates of Francis and Watson's equation above  $\sim 35$  MeV. Below this energy, the estimates of the above semi-empirical equation are lower by a factor of  $\sim 2$  and  $\sim 1.2$  at 10 MeV and 30 MeV, respectively (see Figure 1).

### C. Analysis of excitation functions

The shapes of experimental excitation functions observed in this work for the (p,xn) and (p,pxn) reactions are in good

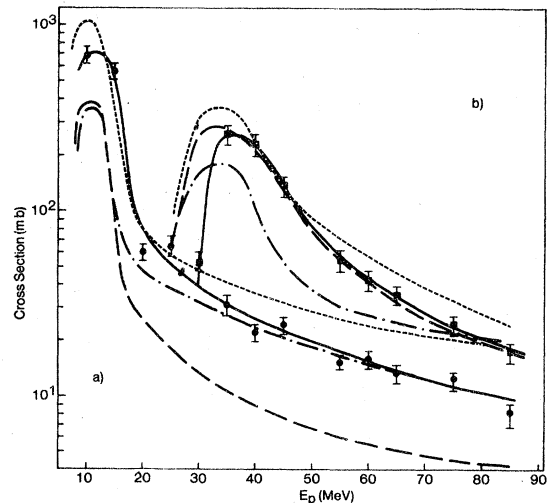


FIG. 2. Comparison of experimental (full-line) and calculated excitation functions.

--- EVA-GDH  
 — exciton model  
 - - - INC-evaporation MECC-7-I4C  
 a) <sup>79</sup>Br(p,n) and  
 b) <sup>79</sup>Br(p,3n) reaction

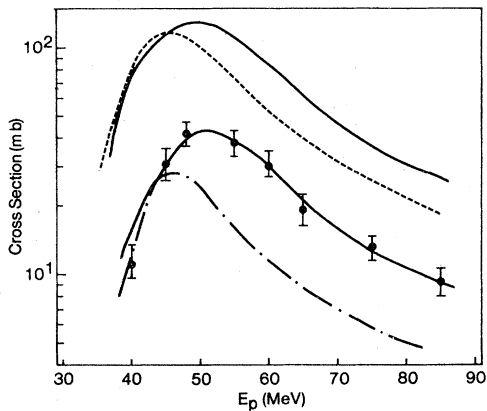


FIG. 3. As Figure 2, for  $^{79}\text{Br}(p,pn)$  reaction.

agreement with those found in earlier studies.<sup>6,9,10,15,20</sup> All three codes gave reasonable reproduction of the shapes of excitation functions. A detailed comparison between the theoretical and experimental excitation functions is summarized below.

$^{79}\text{Br}(p,n)$  - Figure 2a. The position of the maximum of the excitation function is well predicted by all three codes. The experimental cross sections above  $\sim 30$  MeV are well predicted only by the exciton model. The difference between calculated cross sections below about 18 MeV is probably due to the large difference in the reaction cross sections used by the Bertini code on one hand and the other two which use the same reaction cross section.

$^{79}\text{Br}(p,3n)$  - Figure 2b. Absolute values are well predicted by the INC (used to denote MECC-7 evaporation) and EVA-GDH codes. The fit given by the Gadioli code is reasonable.

$^{79}\text{Br}(p,4n)$  - Figure 3. This excitation function is poorly predicted by any of the codes. The INC and exciton model codes over and under-estimate, respectively, by about the same factor. The excitation function is over-estimated by a factor of

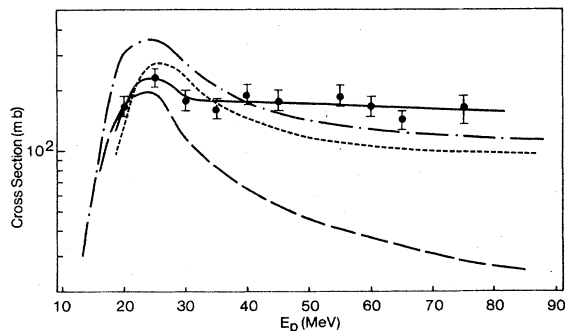


FIG. 4. As Figure 2, for  $^{79}\text{Br}(p,pn)$  reaction.

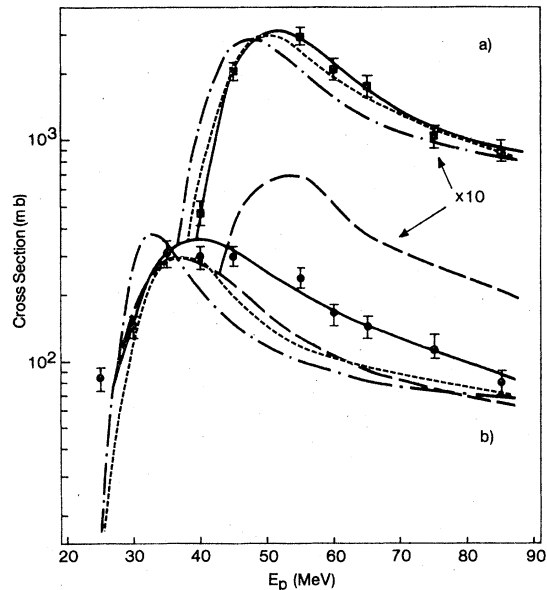


FIG. 5. As Figure 2, for a)  $^{79}\text{Br}(p,p3n)$  multiplied by 10 and b)  $^{79}\text{Br}(p,p2n)$  reaction.

$\sim 2$  by the EVA-GDH.

$^{79}\text{Br}(p,pn)$  - Figure 4. Both the exciton model and INC codes predict this excitation function satisfactorily, even though the former predicts too much compound nucleus. The tail of this excitation function is grossly under-estimated by the EVA-GDH code. The shape of this excitation function suggests that compound-nucleus formation is favored by this model.

$^{79}\text{Br}(p,p3n)$  - Figure 5a. The INC and exciton model codes reproduce this function very well, while prediction by

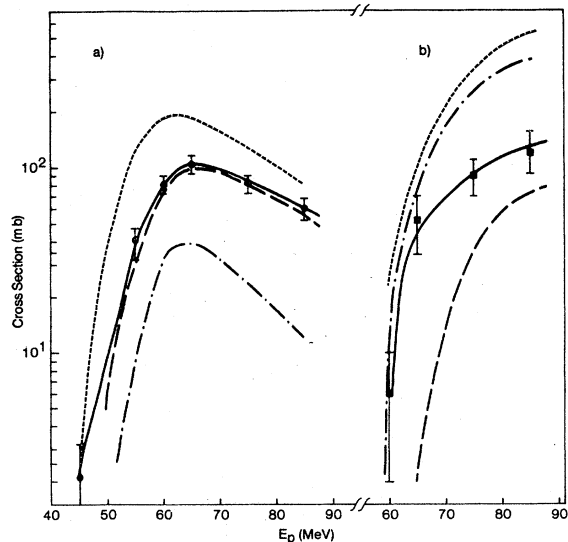


FIG. 6. As Figure 2, for a)  $^{79}\text{Br}(p,p4n)$  and b)  $^{79}\text{Br}(p,p5n)$  reaction.

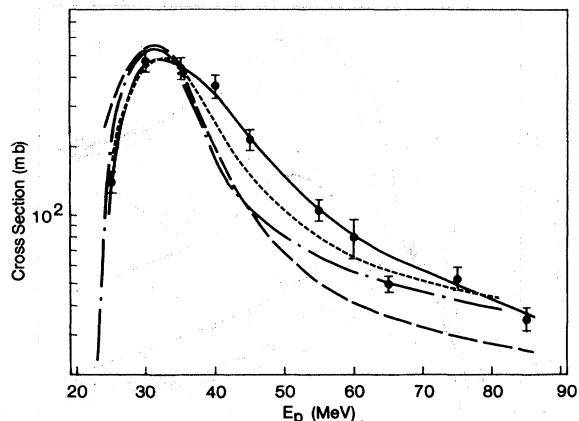


FIG. 7. As Figure 2, for  $^{81}\text{Br}(p,3n)$  reaction.

the EVA-GDH code is lower by a factor of  $\sim 5$ .

$^{79}\text{Br}(p,p2n)$  - Figure 5b. This excitation function is predicted reasonably well by all three codes. It is over-estimated below  $\sim 35$  MeV by the exciton model which shows a shift of the maximum of the excitation function towards lower energies.

$^{79}\text{Br}(p,p4n)$  - Figure 6a. Only the EVA-GDH code gives a good fit. The exciton and INC predict cross sections which are underestimated and over-estimated, respectively by the same factor.

$^{79}\text{Br}(p,p5n)$  - Figure 6b. The experimental results shown are only for one isomer ( $^{74}\text{Br} - t_{1/2} = 41.5$  min.) and thus comparisons are difficult.

$^{81}\text{Br}(p,3n)$  - Figure 7. The three codes

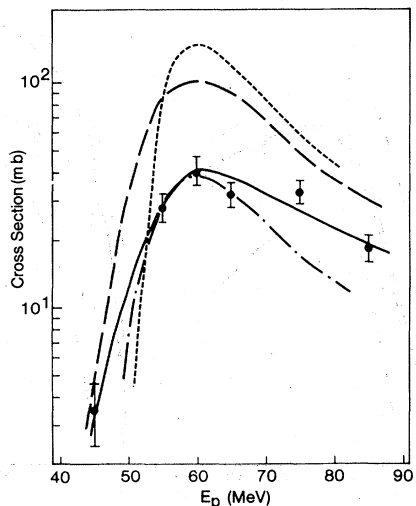


FIG. 8. As Figure 2, for  $^{81}\text{Br}(p,5n)$  reaction.

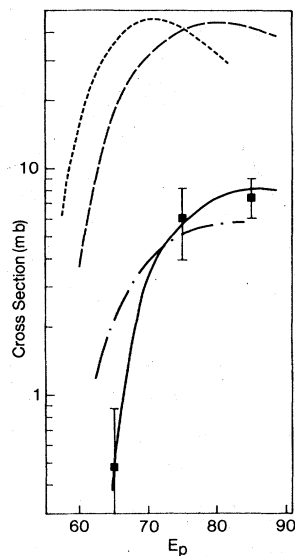


FIG. 9. As Figure 2, for  $^{81}\text{Br}(p,6n)$  reaction.

reproduce this function well, both as to shape and magnitude.

$^{81}\text{Br}(p,5n)$  - Figure 8. The cross sections below  $\sim 70$  MeV are very well predicted by the exciton model and underestimated above it. The amount of compound nucleus is over-estimated by the exciton model and INC codes as evidenced by the shape of the predicted excitation functions. The excitation functions predicted by the EVA-GDH code is too high by a factor of  $\sim 2$ .

$^{81}\text{Br}(p,6n)$  - Figure 9. The exciton model code predicts this function satisfactorily. The INC and EVA-GDH model codes both over-estimate cross sections by a factor of  $\sim 3$ . The latter predicts the shape very well.

$^{81}\text{Br}(p,pn)$  - Figure 10. The INC code

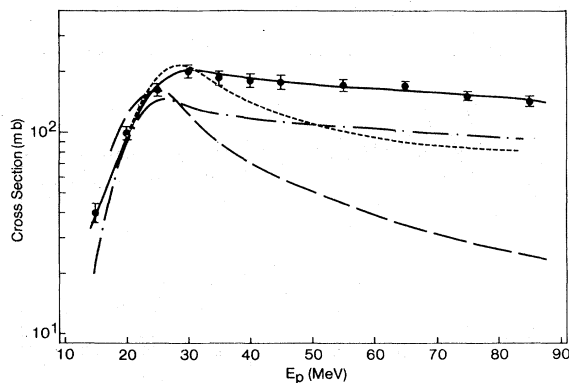


FIG. 10. As Figure 2, for  $^{81}\text{Br}(p,pn)$  reaction.

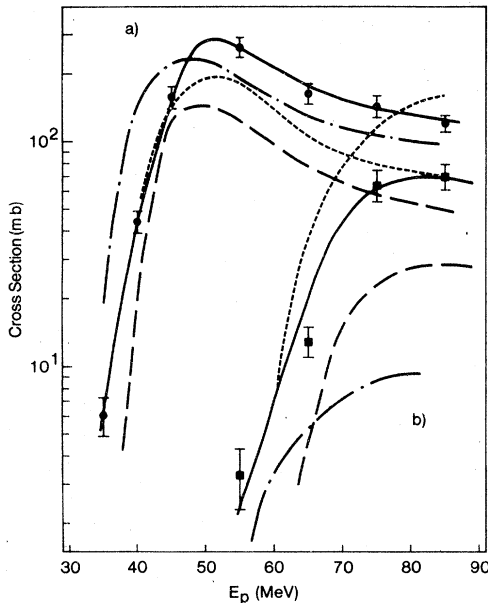


FIG. 11. As Figure 2, for a)  $^{81}\text{Br}(p,p3n)$  and b)  $^{81}\text{Br}(p,p5n)$  reaction.

estimates cross sections which are lower than the experimental ones above the proton energy of  $\sim 40$  MeV. This code along with EVA-GDH predicts too high a compound-nucleus contribution seen from the shape of the predicted excitation function. The prediction of the exciton model is too low above  $\sim 30$  MeV. The latter predicts the shape very well.

$^{81}\text{Br}(p,p3n)$  - Figure 11a. Only the exciton model predicts this excitation function satisfactorily even though it appears to be shifted towards lower energies by  $\sim 7$  MeV. The INC code predicts well only the portion of the excitation

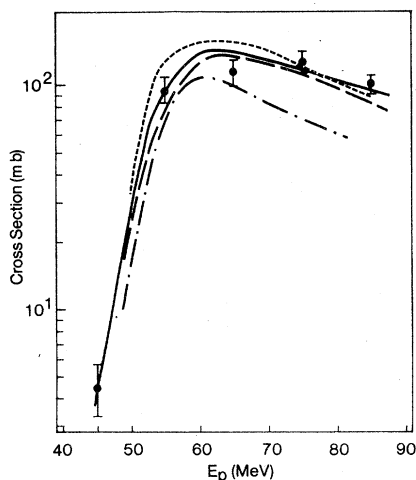


FIG. 12. As Figure 2, for  $^{81}\text{Br}(p,p4n)$  reaction.

function up to  $\sim 45$  MeV. The latter overestimates the contribution from compound nucleus. The EVA-GDH underestimates it by a factor of  $\sim 2.5$  above  $\sim 50$  MeV.

$^{81}\text{Br}(p,p5n)$  - Figure 11b. The excitation function is not well predicted by any of the codes.

$^{81}\text{Br}(p,p4n)$  - Figure 12. The INC and EVA-GDH codes predict this function very well. The exciton model predicts satisfactorily below  $\sim 65$  MeV. The latter overestimates the compound nucleus contribution.

$^{81}\text{Br}(p,p6n)$  All three codes predicted cross sections which are lower by a factor of  $\sim 10$  than the experimental values. Because of this they were not plotted.

#### IV. CONCLUSION

From the observations made above one can conclude that none of the three models was able to predict systematically the experimental excitation functions. However, the INC-evaporation code gives, on an average, the best results. The shape of the excitation functions are almost always reproduced in a satisfactory fashion, whereas magnitudes are often predicted correctly. Whenever they are not, the discrepancy between calculated and experimental results only once exceeds a factor of 3.

Blann's EVA-GDH predicts shapes of the excitation functions quite well except for the  $(p,pn)$  reactions where the shapes are badly predicted. The compound-nucleus contribution is over-estimated in the  $(p,pn)$  excitation functions, making shapes more like  $(p,3n)$  or  $(p,2n)$  excitation functions. It is some indication that the program predicts better the excitation functions with odd number of particles in the exit channel.

Gadioli's exciton model gives several reasonable fits. Whenever discrepancies occur, they do not show any trend. It should be pointed out that the very good fit observed in the tail of  $^{79}\text{Br}(p,n)$  is not surprising since several adjustable parameters used in developing that particular code have been derived by adjusting the calculated cross sections to the tail of  $(p,n)$  experimental excitation functions.<sup>6</sup> The behavior of the excitation functions in the lower energy regions is reasonably well reproduced by the exciton model in the entire energy range, indicating that the approximations introduced in the calculation of the inverse cross sections<sup>6,19</sup> and by neglecting angular momentum<sup>6,19</sup> considerations seem to be justified.

The fact that the combination of the INC and evaporation codes best reproduces the experimental excitation function may



indicate that the long-assumed energy limit of the calculation based on the de Broglie wavelength of the incident particle may not be appropriate. A similar conclusion was reached by Bertini et al.<sup>13</sup>

This work was supported by the National Research Council of Canada (now called National Science and Engineering Research Council).

- \*Present address: Institut de Genie Nucleaire, Ecole Polytechnique, Montreal, PQ, Canada.
- <sup>1</sup>J.M. Blatt and V.F. Weisskopf, *Theoretical Nuclear Physics* (Wiley, N.Y., 1952), pp. 340 and 494.
- <sup>2</sup>N. Metropolis, R. Bivins, M. Storm, A. Turkevich, J.M. Miller, and G. Friedlander, *Phys. Rev.* **110**, 185 (1958).
- <sup>3</sup>H.W. Bertini, *Phys. Rev.* **131**, 1801 (1963).
- <sup>4</sup>K. Chen, Z. Fraenkel, G. Friedlander, J.R. Grover, J.M. Miller, and Y. Shimamoto, *Phys. Rev.* **166**, 949 (1968).
- <sup>5</sup>M. Blann, *Annu. Rev. Nucl. Sci.* **25**, 123 (1975) and references therein.
- <sup>6</sup>E. Gadioli, A.M. Grass Strini, G. Lo Bianco, G. Strini, and G. Tagliaferri, *Nuovo Cimento* **22A**, 557 (1974) and references therein.
- <sup>7</sup>J.J. Griffin, *Phys. Rev. Lett.* **17**, 478 (1966).
- <sup>8</sup>I. Dostrovsky, Z. Fraenkel, and G. Friedlander, *Phys. Rev.* **116**, 683 (1959).
- <sup>9</sup>G.B. Saha, N.T. Porile, and L. Yaffe, *Phys. Rev.* **144**, 968 (1966).
- <sup>10</sup>J.-C. Brodovitch, J.J. Hogan, and K.I. Burns, *J. Inorg. Nucl. Chem.* **38**, 1581 (1976).
- <sup>11</sup>L. Dresner, EVAP-A-FORTRAN Program for Calculating the Evaporation of Various Particles from Exciting Nuclei, Report No. ORNL-TM-196, 1961 (unpublished).
- <sup>12</sup>H.W. Bertini, *Phys. Rev. C* **5**, 2118 (1972).
- <sup>13</sup>H.W. Bertini, G.D. Harp, and F.E. Bertrand, *Phys. Rev. C* **10**, 2472 (1974).
- <sup>14</sup>M.V. Kantelo, Ph.D. thesis, McGill University, 1975 (unpublished).
- <sup>15</sup>M. Dikšić and L. Yaffe, *J. Inorg. Nucl. Chem.* **39**, 1299 (1977).
- <sup>16</sup>M. Blann, *Phys. Rev. C* **17**, 1871 (1978).
- <sup>17</sup>M. Blann, *Phys. Lett.* **B67**, 145 (1977).
- <sup>18</sup>E. Gadioli, E. Gadioli Erba, and J.J. Hogan, *Nuovo Cimento* **A40**, 383 (1977) and references therein.
- <sup>19</sup>E. Gadioli, E. Gadioli Erba, and J.J. Hogan, *Phys. Rev. C* **16**, 1404 (1977).
- <sup>20</sup>J.W. Meadows, R.M. Diamond, and R.A. Sharp, *Phys. Rev.* **102**, 190 (1956).
- <sup>21</sup>M. Dikšić, J.-L. Galinier, H. Marshall, and L. Yaffe, *Int. J. Appl. Radiat. Isot.* **28**, 885 (1977).
- <sup>22</sup>R. Gunnink, H.B. Levy, and J.B. Niday, Lawrence Radiation Laboratory Livermore, Report No. UCID-15140, 1967 (unpublished).
- <sup>23</sup>J.B. Cumming, National Academy of Sciences-Nuclear Science Series, Report No. NAS-NS-3107, 25, 1962 (unpublished).
- <sup>24</sup>J.B. Cumming, *Annu. Rev. Nucl. Sci.* **13**, 261 (1963).
- <sup>25</sup>R. Collé, R. Kishore, and J.B. Cumming, *Phys. Rev. C* **9**, 1819 (1974).
- <sup>26</sup>J.W. Meadows, *Phys. Rev.* **95**, 885 (1953).
- <sup>27</sup>R. Holub, M. Fowler, L. Yaffe, and A. Zeller, *Nucl. Phys.* **A288**, 291 (1977).
- <sup>28</sup>H.B. Blosser and T.H. Handley, *Phys. Rev.* **100**, 1340 (1955).
- <sup>29</sup>R. Collé and R. Kishore, *Phys. Rev. C* **9**, 2166 (1974).
- <sup>30</sup>P.P. Strohal and A.A. Caretto, *Phys. Rev.* **121**, 1815 (1961).
- <sup>31</sup>M. Blann, *Phys. Rev. Lett.* **28**, 757 (1972).
- <sup>32</sup>Code name assigned by us to the Blann code.
- <sup>33</sup>W.D. Meyers and W. Swiatecki, University of California, Berkeley Radiation Lab., Report No. UCRL-11980, 1965 (unpublished).
- <sup>34</sup>A.G.W. Cameron, *Can. J. Phys.* **36**, 1040 (1958).
- <sup>35</sup>A.H. Wapstra and N.B. Gove, *Nucl. Data* **9**, Nos. 4-5 (1971).
- <sup>36</sup>P.E. Nemirovski and Yu. V. Adamchuk, *Nucl. Phys.* **39**, 551 (1962).
- <sup>37</sup>R. Hofstadter, *Rev. Mod. Phys.* **28**, 214 (1956).
- <sup>38</sup>D.J. Hughes and R.B. Schwartz, Neutron cross sections, 2nd ed., Report No. BNL-325, 1958 (unpublished).
- <sup>39</sup>L. Beretta, C. Villi, and F. Ferrari, *Nuovo Cimento* **12**, 5499 (1954).
- <sup>40</sup>W.N. Hess, *Rev. Mod. Phys.* **30**, 368 (1958).
- <sup>41</sup>V.F. Weisskopf, *Phys. Rev.* **52**, 295 (1937).
- <sup>42</sup>M. Blann, *Nucl. Phys.* **A213**, 570 (1973).
- <sup>43</sup>G.S. Mani, M.A. Malkanoff, and I. Iori, Centre d'Etudes Nucleaires de Saclay, Report No. CEA 2379, 1963 (unpublished).
- <sup>44</sup>F.C. Williams, *Phys. Lett.* **B31**, 184 (1970).
- <sup>45</sup>N.F. Francis and K.M. Watson, *Am. J. Phys.* **21**, 659 (1953).
- <sup>46</sup>R. Collé and R. Kishore, *Phys. Rev. C* **9**, 981 (1974).
- <sup>47</sup>P.P. Urone, L.L. Lee, Jr., and S. Raman, *Nucl. Data Sheets* **9**, 229 (1973).
- <sup>48</sup>F.E. Bertrand and R.L. Auble, *Nucl. Data Sheets* **19**, 507 (1976).
- <sup>49</sup>L.R. Greenwood, *Nucl. Data Sheets* **15**, 289 (1975).
- <sup>50</sup>P.P. Urone and F.E. Bertrand, *Nucl. Data Sheets* **15**, 107 (1975).
- <sup>51</sup>D.J. Horen and M.D. Lewis, *Nucl. Data Sheets* **16**, 25 (1975).
- <sup>52</sup>H. Schmeig, R.L. Graham, J.C. Hardy, and J.S. Geiger, *Nucl. Phys.* **A233**, 63 (1974).
- <sup>53</sup>R.L. Auble, *Nucl. Data Sheets* **14**, 119 (1975).
- <sup>54</sup>S. Raman, N.B. Gove, J.K. Dickens, and T.A. Walkiewicz, *Phys. Lett.* **B40**, 89 (1972).